An Approach for Contact Stress Mapping in Joints and Concentrated Contacts

M.B. Marshall[a], R. Lewis[a], B.W. Drinkwater[b], and R.S. Dwyer-Joyce[a]

[a]Department of Mechanical Engineering,
Mappin Street, University of Sheffield, Sheffield S1 3JD, UK
[b]Department of Mechanical Engineering,
Queen's Building, University of Bristol, Bristol BS8 1TR, UK

Abstract

The measurement of pressure at a contact in a machine part is important, because it is frequently contact stresses which lead to failure by seizure, wear, or fatigue. Whilst the interface might appear smooth on a macro-scale, it consists of regions of asperity contact and air gaps on a micro-scale. The reflection of an ultrasonic pulse at such a rough contact can be used to give information about the contact conditions. The more conformal the contact, the lower the proportion of an incident wave amplitude that will be reflected. In this paper, this phenomenon has been used to produce maps of contact pressure at machine element interfaces. An ultrasonic pulse is generated and reflected at the interface, to be received by the same piezo-electric transducer. The transducer is scanned across the interface and a map of reflected ultrasound, a c-scan, is recorded. The proportion of the wave can be used to determine the stiffness of the interface. Stiffness correlate qualitatively with contact pressure but unfortunately there is no unique relationship. In this work, two approaches have been used to obtain contact pressure; firstly be using an independent calibration experiment, and secondly be using experimental observations that stiffness and pressure are linearly related. The approach has been used in three cases; a series of press fitted joints, a wheel-rail contact, and a bolted joint.

Introduction

The interaction of machine components under loading is an integral part of engineering design. It results in a mechanical contact and associated stress distribution, which may be an initiation point for failure modes such as fatigue, fretting, or wear. Frequently contact stresses are of high magnitude and occur over small regions. This means they are difficult to measure and also difficult to model by, for example, finite element methods.

It is possible to use pressure sensitive films or micro-transducers to sense load contact pressure changes. However, they typically have a low spatial resolution and alter interface properties. Surface roughness plays an important part in contact mechanics, and such a film will alter the contact and associated pressure distribution.
The theoretical prediction of contact stresses in machine components is also problematic. There are only analytical models for smooth surfaces of regular geometry in elastic contact. Finite and boundary element methods tend to be used where these assumptions are not valid. However, the models require very fine meshing in the contact region and the current state of computing power still cannot incorporate surface roughness effects.

In this study the reflection of ultrasound is used to investigate how real engineering components contact. It is a non-intrusive technique preserving the mechanics of the contact. The concept is simple; an acoustic wave bounces back from a rough surface contact. The higher the contact load, the more conformal will be the contact and hence more of the wave will be transmitted. However, there are many practical aspects concerning the analysis of reflected signals and how the method can be applied to machine components.

Reflection of Ultrasound from an Interface

When an ultrasonic wave is focused on a boundary between two perfectly bonded materials some of it is reflected back (Tattersall, 1973). A reflection coefficient, *R*, the proportion of the signal amplitude reflected from the interface may be defined as:

$$R_{12} = \frac{z_1 - z_2}{z_1 + z_2} \tag{1}$$

where *z* is the acoustic impedance (the product of density and wave speed through the material), and the subscripts 1 and 2 denote the material above and below the interface respectively. If a wave is travelling through a metal and is incident at an air interface, virtually all the signal will be reflected back. This is due to the low impedance of the air relative to the metal.

Reflection of Ultrasound from a Rough Surface Contact and Interfacial Stiffness

In reality, real surfaces are not smooth and consist of randomly shaped asperities. Two surfaces pressed together will contact at asperity tips and trap tiny pockets of air, as shown in Figure 1. When the ultrasonic pulse strikes the interface it will pass through regions of asperity contact and be reflected back at air gaps.

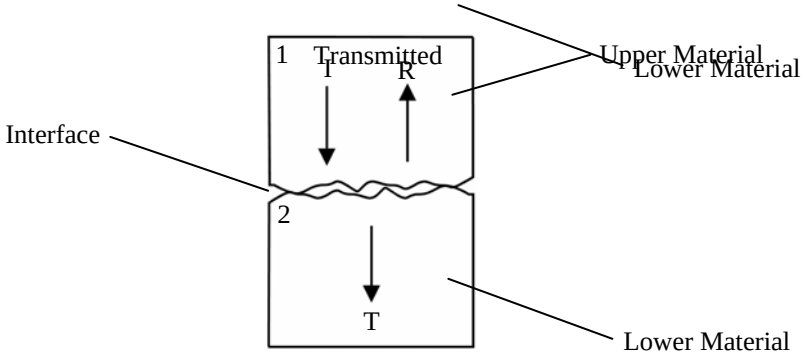

Figure 1: *'Contact of a Real Engineering Surface.'*

If the incident ultrasonic wavelength is of similar magnitude to the air gaps, scattering occurs. Alternatively, when the wavelength is long in comparison to the gaps, the interface as a whole behaves as a reflector. Kendall and Tabor (1971) investigated this case and found reflection to be governed by the *spring* behaviour of the interface. The reflection coefficient can be defined in terms of the interfacial stiffness, *k*:

$$R_{12} = \frac{z_1 - z_2 + \mathrm{i}\omega(z_1 z_2 / k)}{z_1 + z_2 + \mathrm{i}\omega(z_1 z_2 / k)} \quad (2)$$

where ω is the angular frequency of the wave ($\omega = 2\pi f$), z the impedance, and i the imaginary component (Tattersall, 1973).

The property interfacial stiffness originates from the spring model of contacting surfaces. The stiffness k (expressed per unit area) is defined as the change in nominal contact pressure required to cause unit approach of the mean lines of the surfaces (Thomas and Sayles, 1977).

Application of the Spring Model

Drinkwater et al. (1996) assessed the applicability of the spring model to ultrasonic reflection data from a series of rough surface interfaces of varying stiffness. They demonstrated that the spring model may be applied to reflection data from typical machined surfaces up to ultrasonic frequencies of ~30 MHz. They also found that as R tends to zero or unity the spring model becomes unstable, showing a deviation from frequency independence within the stiffness data.

This spring model approach can therefore be used to determine the stiffness of a contact. Contact stiffness alone is a useful parameter as it defines the dynamic response of the machine element. A contact stiffness map will also qualitatively indicate regions of high and low conformity (and hence pressure). However, contact pressure and hence stress is more useful to the designer. The analytical determination of contact pressure from stiffness measurements is not straightforward because stiffness is a function of the number and size of asperity contact regions as well as their proximity. Some kind of rough surface contact model is required to provide this link (Dwyer-Joyce et al., 2001). However, experiments have shown that at low pressure the relationship between contact pressure and interfacial stiffness may be approximated as linear (Drinkwater et al., 1998).

Further, calibration methods (Dwyer-Joyce et al., 1998, Drinkwater et al., 1998) have been used to find the pressure-stiffness relationship that is subsequently applied to the measured data.

Ultrasonic Scanning Apparatus

The ultrasonic equipment consists of an ultrasonic transducer, an oscilloscope, and an Ultrasonic Pulse-Receiver (UPR). A schematic of the equipment set-up is shown in Figure 2. In this work a 10 MHz central frequency focusing transducer was used. It emits useful energy in the frequency band 4-14 MHz, and has a concave lens to focus the generated sound waves. Water is required as a couplant between the probe and specimen, as ultrasound is rapidly scattered in air. The transducer operates on 'pulse-echo' mode, receiving the reflected pulse back from the interface. Once received, the pulse is amplified and stored on a digital oscilloscope. The amplitude of the reflected voltage signal is downloaded from the oscilloscope to the PC.

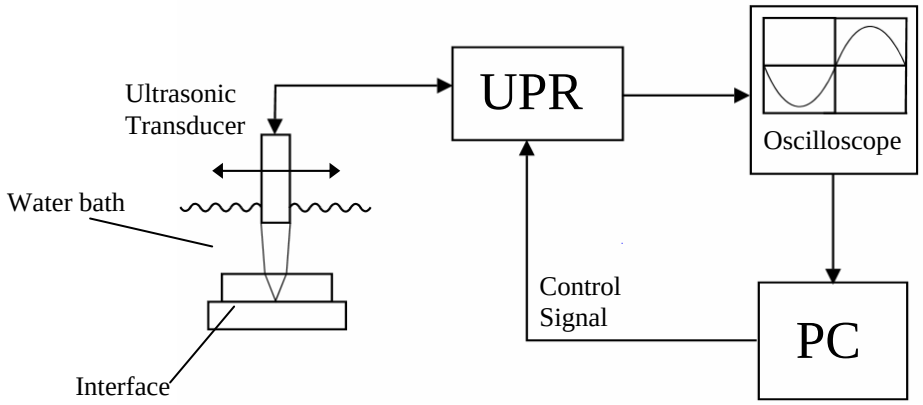

Figure 2: *'A Schematic of the Equipment Set-Up.*

Ultrasonic Signal Processing

The measured reflected signal is lower than the emitted pulse for two reasons. Firstly, at the interface some of the incident signal is transmitted, and secondly attenuation occurs as the wave travels to and from the contact. The reflection coefficient is the fraction of ultrasound incident at the interface that is reflected from it, and is required to calculate interfacial stiffness. To find this quantity a reference signal is used which separates ultrasonic attenuation from interface transmission. The reference signal is the amplitude of the reflected voltage from a point of no contact, since all ultrasound is reflected from a solid-air boundary. It is determined by either finding a point of no contact on the interface, or by removing the opposing specimen. The reflection coefficient is calculated by dividing the reflected voltage from the contact by the reference value.
The reflection coefficient is then converted to an interfacial stiffness using Equation 2 from the spring model. In applying Equation 2, the centre frequency of the ultrasonic probe is used, as the reflected signal amplitude occurs at this value. For the 10 MHz probe used in these experiments the centre frequency is 8.8 MHz. An appropriate calibration is performed to relate contact pressure to interfacial stiffness for the rough surface pair. A simple schematic of the calibration rig is shown in Figure 3.

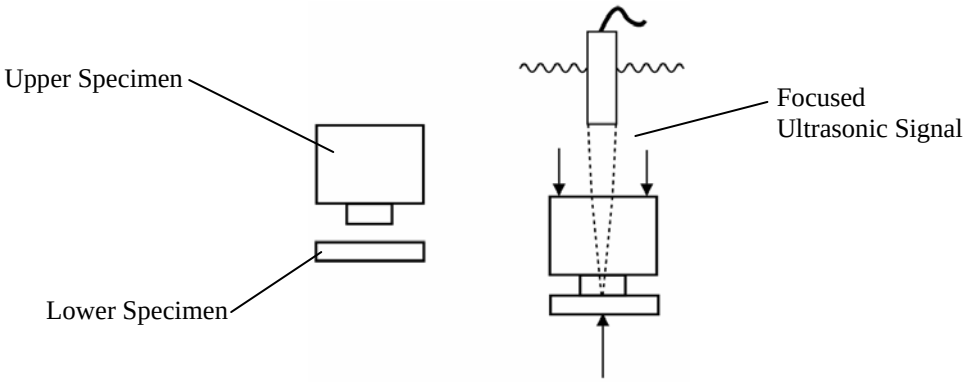

Figure 3: *'Calibration Specimens and Experiment.'*

The calibration specimens shown are made from the same material and to the same surface roughness as the contacting components the calibration is required for. They are pressed together at a series of known loads, and single point ultrasonic reflection

measurements made. As the interface between them is flat and of known geometry, the contact pressure at a given load can be determined. A reference trace is taken with the lower disc absent. Reflection coefficient and interfacial stiffness (using Equation 2) can then be calculated at each contact pressure and a calibration curve plotted.

Application to Three Machine Element Contacts

The approach described above has been applied to three different engineering applications. In each case an ultrasonic transducer has been scanned across the loaded interface and the reflection determined. This has been used to create stiffness maps. These have been converted to pressure distributions by means of a calibration curve.

Interference Fit Interface Pressure

The interference fit specimens were constructed from EN24 steel (see Figure 4). The components were lathe finished to R_a = 1.5 μm. A hole is drilled into the shaft as a reference point for the ultrasonic signal, its use will be explained further on.

Figure 4: *'A Specimen Interference Fit. Disassembled Showing the Reference Hole, and in its Assembled State.'*

The specimen interference fits examined in this series of experiments are shown in Table 1. Dimensions of shafts and sleeves are given as well as interferences. Specimens were assembled using press fitting and shrink fitting techniques. Press fitting was performed unlubricated on a 60 Tonne industrial press, whilst shrink fitting was achieved by cooling the shaft in liquid nitrogen until it could be dropped into the sleeve. The 0.025, 0.05, and 0.075 mm fits are identical apart from the magnitude of their interference. Similarly, the two 0.03 mm interference specimens have identical radial geometry. The 0.03 mm shrink fit was of reduced length compared to its pressed counterpart due to mechanical issues when shrink fitting with liquid nitrogen. It was found that if the sleeve was any longer the shaft would expand and seize during assembly.

	Shaft	Sleeve

Diametral Interference (mm)	Construction Method	O.D. (mm)	Length (mm)	O.D. (mm)	Length (mm)
0.025	Press	50	120	80	90
0.050	Press	50	120	80	90
0.075	Press	50	120	80	90
0.030	Press	40	70	60	50
0.030	Shrink	40	30	60	20

Table 1: *'Interference Fit Specimen Geometry.'*

Scanning of the Interface

The interference fit specimens were mounted on a vee block within a modified C-scanning tank and immersed in water. A PC interfaces the ultrasonic equipment and scanning tank. Line scans were taken around the interface at 10 degree intervals, with ultrasonic readings made every quarter of a millimetre. Figure 5 shows the interface scanning, with the 10 MHz probe positioned to focus ultrasound on the interface. When scanning, the fifth average of the reflected voltage signal from the interface was recorded.

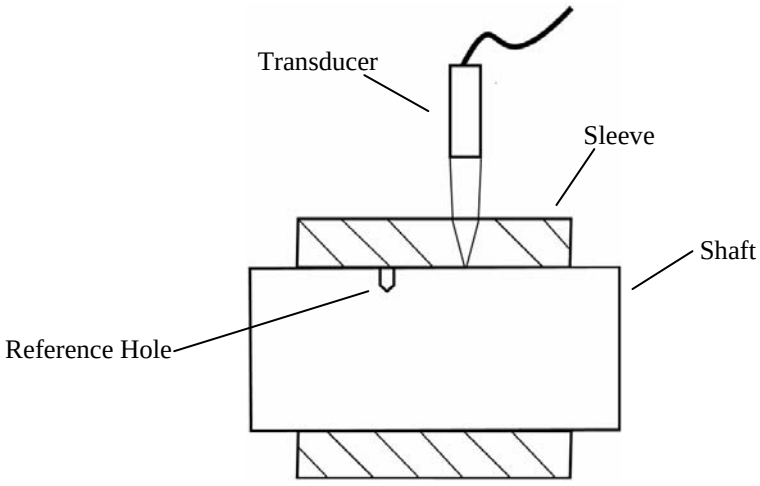

Figure 5: *'Interface Scanning.'*

A reference scan was taken for each interference fit specimen. This involved scanning the sleeve before the shaft was inserted, which gave a solid-air interface, meeting the requirement for reflection coefficient calculation. Radial symmetry was found when taking the reference traces; a single reference line could therefore be used for each specimen. Figure 6a shows the reference for the 0.025 mm fit, with the loss in signal strength at the edge explained by Figure 6b. As shown, close to the edge of the sleeve some of the ultrasonic signal strength is lost whilst focusing. The reference hole in the shaft was used to check the reference had not changed once the fit had been assembled.

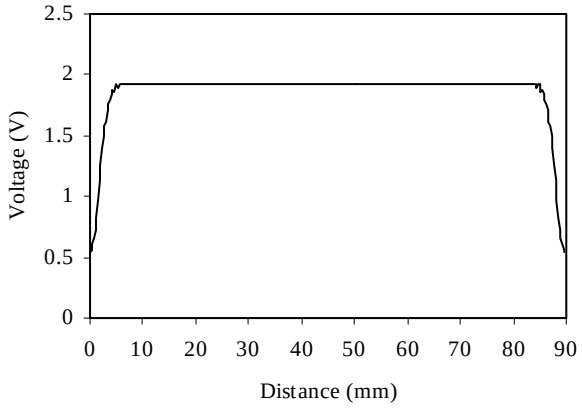

Figure 6a: *'Reference Scan for Specimen 1.'*

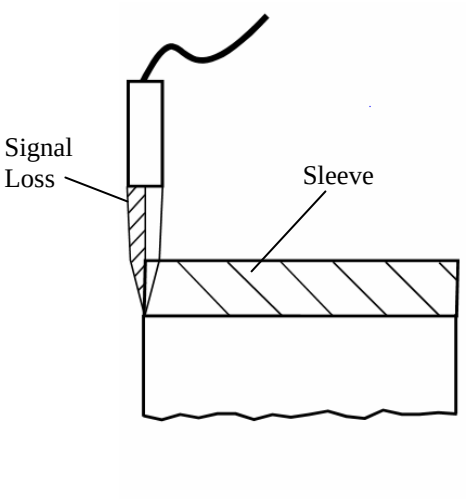

Figure 6b: *Signal Loss at the Sleeve Edge.'*

A calibration experiment was performed to relate interfacial stiffness to contact pressure for the interface. This gave the calibration points shown on Figure 7, approximated to the linear relationship $p = 60.14K$.

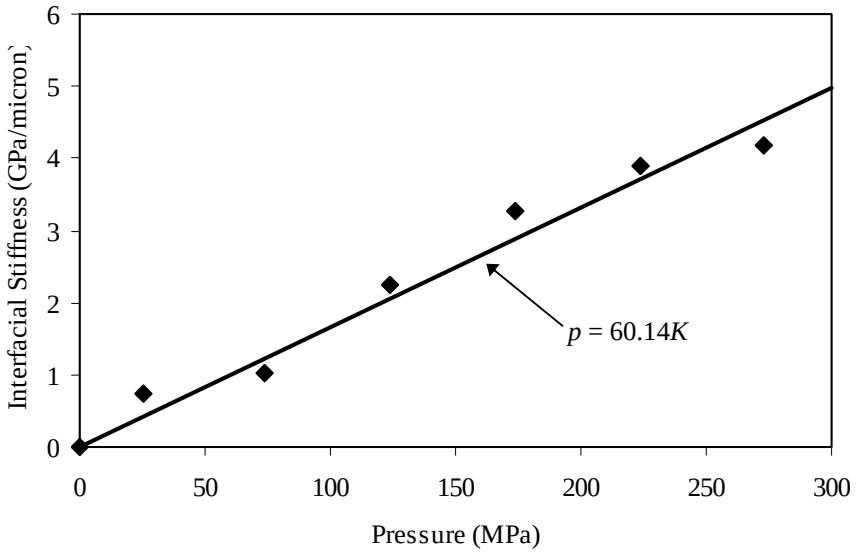

Figure 7: *'Calibration Results.'*

Interface Pressure Maps

Contact pressure maps for the interface of each interference fit were constructed using the reflected voltage data. Figure 8 shows the contact pressure map for the 0.025 mm fit. Only a single map is shown, as the general trends observed were the same for all the specimens.

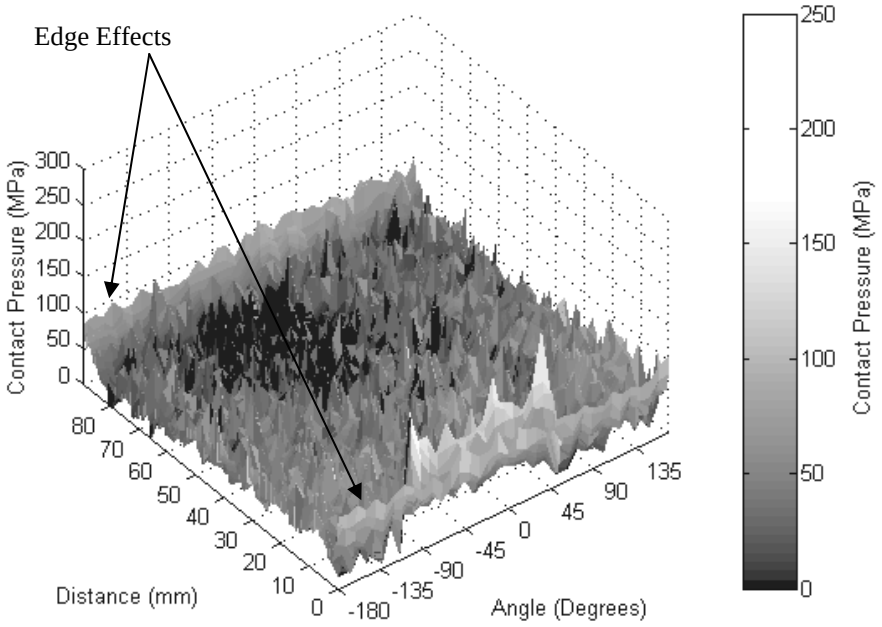

Figure 8: *'Contact Pressure Map for the 0.025 mm Fit.'*

As shown, the contact pressure along the length of the interface was not constant. However, as may be expected there was a high degree of radial symmetry. The contact pressure rose to a maximum near the edges of the interface and showed continuous variation about a mean value in the inverted plateau away from the edge effects. In some of the specimens anomalies were observed in the interface pressure map. Inspection of the reflected ultrasonic signal at these points showed the anomaly was likely attributable to surface damage. Upon disassembly of the specimens this was indeed found to be the case (Lewis et al. 2002).

The contact pressures recorded for the specimens can be compared to the Lamé theory for interference fits (see for example Benham et al., 1996). The theory neglects stress concentration effects, or otherwise, at the edges of an interference fit. In essence the theoretical solution is only applicable to an interference fit of infinite length. The interference fits used in this series of experiments all had finite length. Therefore, to quantitatively compare to theory, the average pressure for the interference fits within the described inverted plateau was used. Figure 9 compares the average pressure of the interference fits to theory; as shown there is good correlation.

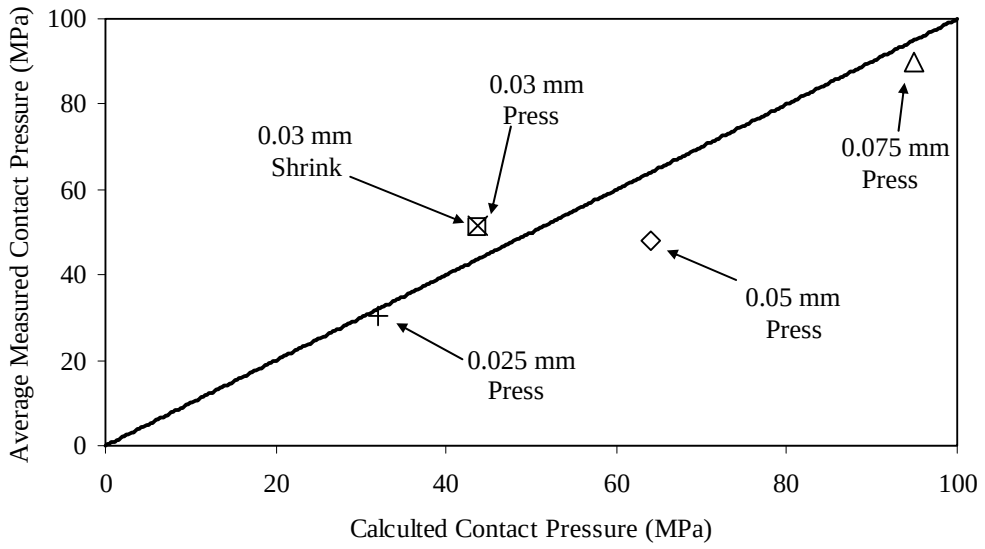

Figure 9: *'Comparison of Average Measured and Theoretical Interface Pressure.'*

The Lamé theory predicts a uniform contact pressure distribution at the interface. This is not consistent with the measured pressure maps of the interference fit specimens. Figure 10 shows line scans from the 0.025, 0.05, and 0.075 mm interference fit specimens. As shown the contact pressure along the interface was not constant. Even if the edge effects are disregarded, variation in pressure is still observed within the inverted plateau. This is attributable to the roughness variation on the specimen surfaces at the interface.

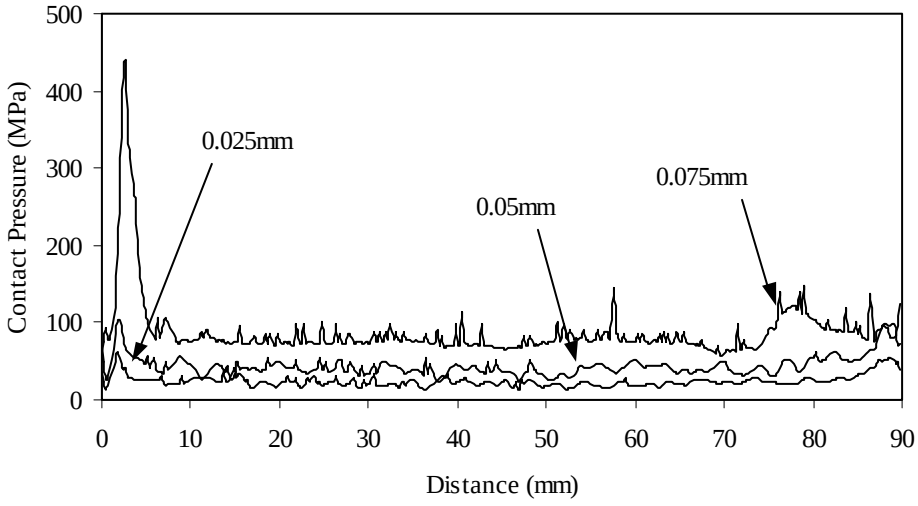

Figure 10: *Line Scans of the 0.025, 0.05, and 0.075 mm Fits.'*

Figure 10 also clearly shows the observed increase in contact pressure at the edges of the interface. For most of the specimens the pressure was seen to gradually rise and then fall. Checks on the signal and inspection of the specimens showed that the reduced reflection was indeed due to an increased contact. Whilst it may seem reasonable for the pressure to rise at the edges of the fit, especially when stress concentration factors are considered, the subsequent decrease is less easy to comprehend. Upon investigation it was found that the de-burring method in the

manufacturing process left a slight internal chamfer on the sleeve, which caused the observed reduction.

Investigation of a Wheel-Rail Contact

Both railway track and wheel durability along with their vibrational response depends on the size and stress distribution within the contact. There are currently no experimental methods for determining these, and emphasis is placed on numerical models of the contact. Sample sections cut from wheel and rail components have been used to evaluate the ultrasonic reflection based method.

Specimen Geometry and Loading

Sample wheel and rail specimens were cut from an actual wheel and rail. Care was taken when preparing the specimens not to damage the surface geometry or finish; this ensured the mechanical contact between the two was preserved for the experiment. Figure 11 shows the loaded wheel and rail specimens being scanned. The 10 MHz transducer is mounted in a water-bath, and so positioned to focus the ultrasonic signal on the interface between the pieces of wheel and rail. In this series of experiments the reference trace was taken from an area to the side of the contact. The wheel-rail specimens were loaded in the range 20-80 kN, this is typical of the loading these specimens would expect during use.

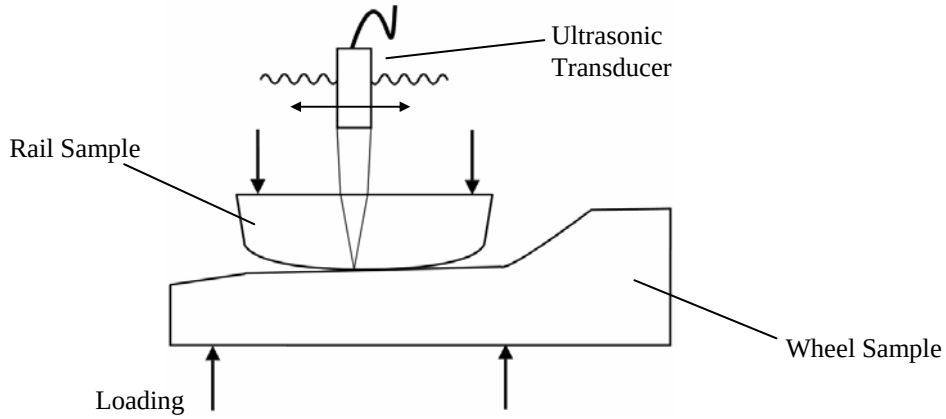

Figure 11: *'Scanning of the Wheel-Rail Contact.'*

Contact Pressure Distribution

Figure 12 shows the contact pressure maps of the wheel-rail contact at 20, 40, 60, and 80 kN. They were generated using the reflected voltage data from the scans along with the calibration procedure previously outlined. Also marked on the Figure is the predicted Hertzian contact patch for the two specimens (see for example calculation Johnson, 1985).

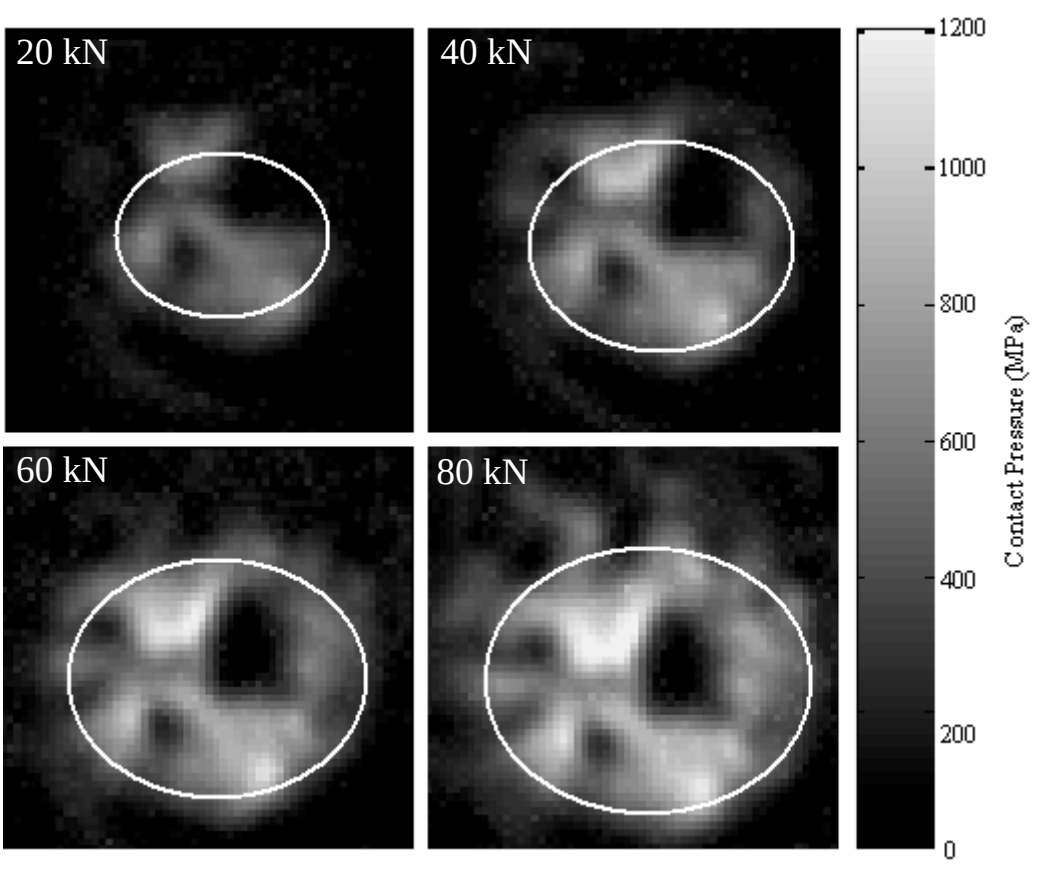

Figure 12: *'Wheel-Rail Contact Pressure Maps.'*

As shown there is good geometric correlation between the measured and predicted data. It should be noted that both the wheel and rail specimens were worn, this causes the observed fragmentation of the contact when compared to the Hertz solution. Due to the reduced contact area attributable to wear, the maximum pressure in the contact is also higher than that predicted by theory (see Table 2).

Load (kN)	Max. Hertz Pressure (MPa)	Max. Measured Pressure (MPa)
20	625	726
40	787	1020
60	901	1184
80	992	1296

Table 2: *'Comparison of Measured and Predicted Maximum Contact Pressure.'*

A check can be made on the validity of the calibration procedure. The wheel and rail specimens were loaded together hydraulically and scanned at a series of known loads. The interface loading was then determined by means of summing the pressure over the area of the contact patch. For a given scan these two values should be the same. Figure 13 shows the comparison for all the loads at which interface scanning was performed on the specimens. As shown, the correlation is good between the two methods for determining total load, validating the calibration procedure.

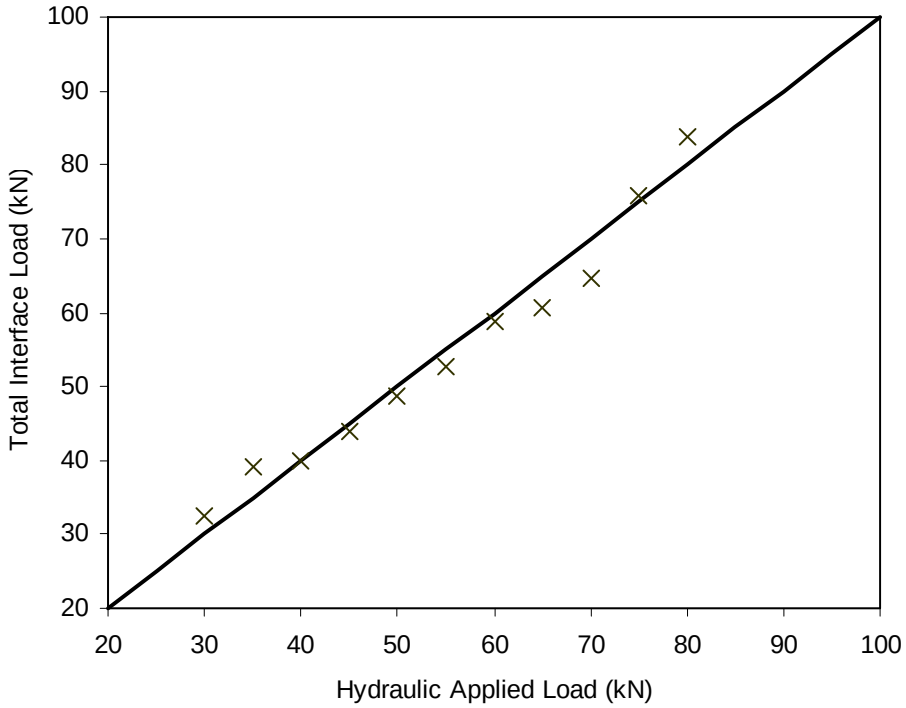

Figure 13: *'Applied and Measured Load Comparison.'*

Load Distribution in a Bolted Joint

In designing bolted joints an important consideration is the effective area of the contact pressure in the joint. Joint member stiffness calculations (see for example Shigley, 2001) use a pressure-cone approach to determine the spread. Figure 14 shows the cone geometry using a half apex angle, α.

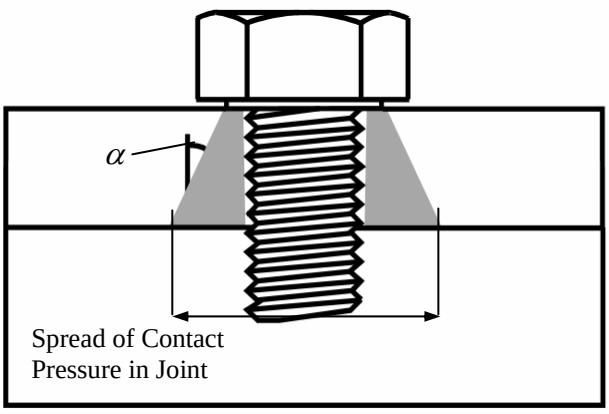

Figure 14: *'Pressure-Cone Method for Determining Spread of Contact Pressure in a Bolted Joint.'*

In order to provide a study of the contact pressure in a bolted joint, a simple specimen consisting of a plate bolted to a base was manufactured from EN24 steel (see Figure 15a). The bolt was torqued and the interface scanned using ultrasound (as shown in Figure 15b). Scans were carried out at torques ranging from 30 to 70 Nm at 10 Nm increments.

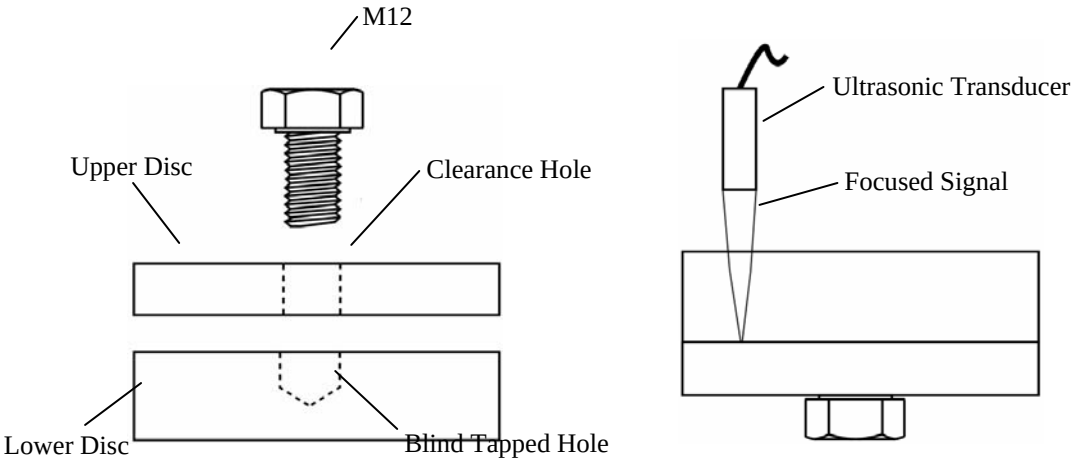

Figure 15: *'Bolted Joint Specimen (a) Geometry and (b) Scanning Technique.'*

A reflection coefficient scan is shown in Figure 16 at a torque of 50 Nm, it should be noted that edge effect calibration has not been carried out. As can be seen the contact pressure distribution is non-symmetrical. The darker bands that can be seen on the plot indicate that the peak pressure occurs away from the edge of the bolt hole, as lower reflection coefficient indicates higher pressure. This is a general trend observed for all the different torques at which scanning was performed. It was also seen that whilst the intensity of the contact increased with applied torque, the overall spread of the distribution remained unchanged.

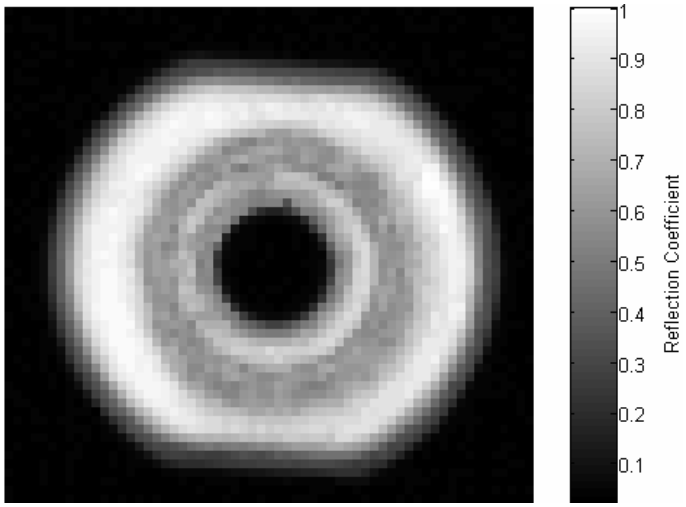

Figure 16: *'Reflection Coefficient Scan at 50Nm.'*

Figure 17 shows a line scan taken from the 50 Nm scan, here the reflection coefficient data has been converted to interfacial stiffness. Using this data the spread of the contact may be determined using the pressure-cone approach. A value of 41° was calculated for this plot.

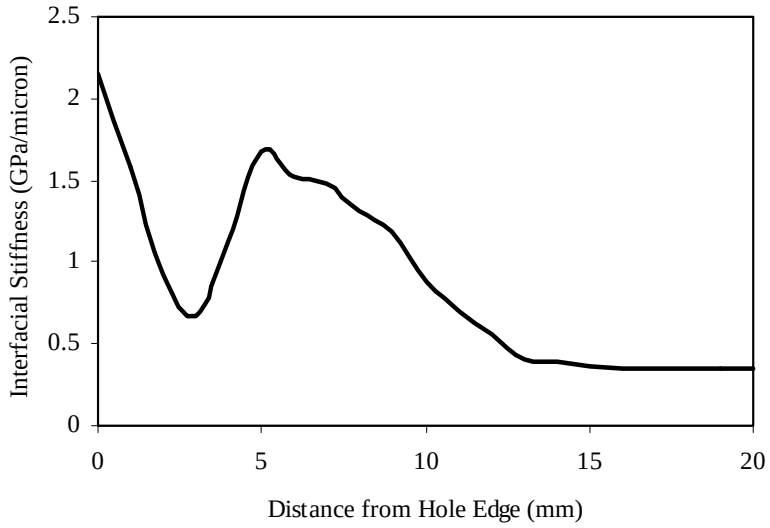

Figure 17: *'Line Scan from 50 Nm Plot.'*

The value calculated here may be compared to those determined in previous studies (Table 3).

Originator	Technique	Half Apex Angle
Present Study	Ultrasonic Scanning	$\alpha = 41°$

Shigley (2001)	Elasticity	$\alpha = 30°$
Osgood (1979)	Elasticity	$25° \leq \alpha \leq 33°$
Ito (1977)	Single Point Ultrasonic Measurement	$\alpha \sim 70°$
Fernlund (1970)	Elasticity	$\alpha = 45°$
Shibahara (1969)	Elasticity	$\alpha = 45°$
Mitsunaga (1965)	Elasticity	$\alpha = 45°$

Table 3: *'Contact Pressure Spread in a Bolted Joint.'*

It should be noted that a number of drawbacks exist in the work of Ito (1977). The measurements were taken at discrete points so no overall picture of the contact pressure could be obtained; data had to be extrapolated near the bolt hole and it was impossible to accurately determine low contact pressures. With the extrapolation used, the peak pressure occurred at the edge of the bolt hole. This is shown not to be the case in this study, and also by the finite element work of Ziada (1980) that showed the peak pressure occurred as a ring under the edge of the bolt head.

Qualitative measurements showed that the contact pressure distribution varied considerably with plate material, the surface finish of the joint surfaces and to some extent the plate thickness. It was also shown that α values could be as high as 70°. Clearly there is no satisfactory means to determine α values and a quantitative method for assessing how α varies with material properties and joint geometry is required.

Discussion

The work described has shown a procedure whereby measurement of ultrasonic c-scans at an interface can be used to determine contact pressure at the interface. This provides a useful method to look into contacts that has not been available before. There are a number of technological issues associated with the method that means that it is not suitable for use on all types on machine element contacts. These issues are reviewed here.

Transducer Coupling and Scanning

Firstly, the transducer must be coupled to the material through which it is looking. De-ionised water is commonly used for this function as the air bubbles present in normal water scatter the ultrasonic signal. This requires either immersion of the specimen, or construction of a water bath around the scanning area. It is not feasible to use a transducer mounted directly onto component back face coupled with a standard gel-couplant. When the transducer is moved to a new location during the scan, the thin couplant layer is not repeatable. The incident signal amplitude thus varies. It is difficult to separate the variance in reflection cased by this change in incident signal from the required change in the reflected signal. It is possible to use other liquid couplants, or perhaps transducers that transmit ultrasound through air (Bhardwaj, 2000), these are however still at an early stage of development. However

it is important that liquid does not penetrate into the interface being measured; a liquid at the interface increases the acoustic transmission and would need to be considered in the analysis to determine contact pressure from reflection coefficient.

Another difficulty associated with the scanning technique is that the incident wave must strike the interface normally. This work was performed on a scanning tank with 2-axis automation. Thus limiting the work to interfaces perpendicular to the transducer, with constant material thickness between the top surface of the specimen and interface. Using a 3-axis scanning tank with automated transducer rotation may alleviate such difficulties. However, such a system would increase both complexity and cost significantly.

As previously shown, a reference trace is required to employ this technique. This can prove a problem when scanning specimens without an area out of contact, or which cannot be readily disassembled.

Spatial Resolution and Edge Effects

The spatial resolution of the technique is limited by the frequency of the ultrasound used. Typically a 10 MHz transducer can be focused to a spot diameters of ~0.2 mm. An improved resolution is obtainable by using higher frequencies; but these higher frequencies tend to be attenuated to a greater extent. The finite spot size can lead to a blurring of the measurement, as part of the reflected signal comes from either side of the point under examination. This can prove to be a particular problem for small contacts with rapidly changing pressure profiles. In this work all the contacts are relatively large with comparatively low pressure gradients, hence the effects of the spot size are negligible. It is possible to de-convolve results to take account of the finite spot size (Hodgson, 2002). But, inherent numerical inaccuracies tend to preclude this approach from all but geometrically simple contacts. Further, care must be taken when scanning near the edge of a specimen. The associated signal loss must be accounted for by the reference, to avoid misinterpretation of the results at these points.

Conclusion

Ultrasonic reflection from an interface provides a method for determining the conditions at machine element contacts. The approach is based on the fact all surfaces are rough. The ultrasonic signal reflects from air gaps and passes through regions of solid contact within a rough surface interface. The reflection depends on the stiffness of the interface. For a given rough surface pair a calibration may be performed relating stiffness to contact pressure.

The technique is useful for scanning many different engineering contacts. In this case it has been applied to determine both contact pressure magnitude and distribution.

Examination of the results from the three studies shows good correlation to established theory.

The spatial resolution of the ultrasonic transducer is an issue when investigating small contacts with rapid pressure changes. In this study such contacts were not probed, with the technique applied to large contacts containing only gradual pressure changes.

De-convolution of measured results is possible, but because of numerical errors has only limited applicability.

The method is therefore best applied to large contacts, as shown by the examples in this work.

References

Benham, P.P., Crawford, R.J., 1996, Armstrong, C.G., *Mechanics of Engineering Materials*, Longman, pp367-395.

Bhardwaj, M.C., Neeson, I., Stead, G., 2000, "Introduction to Contact-Free Ultrasonic Characterization and Analysis of Consolidated Materials", Second Wave Systems, Boalsburg PA USA.

Drinkwater, B.W., Dwyer-Joyce, R.S., Cawley, P., 1996, "A Study of the Interaction between Ultrasound and a Partially Contacting Solid-Solid Interface", *Proceedings of the Royal Society Series A*, Vol. 452, No. 1955, pp. 2613-2628.

Dwyer-Joyce, R.S., Drinkwater, B.W., and Quinn, A.M., 2001, "The Use of Ultrasound in the Investigation of Rough Surface Interfaces", *ASME Journal of Tribology*, Vol. 123, pp 8-16

Dwyer-Joyce, R.S., Drinkwater, B.W., 1998, "Analysis of Contact Pressure Using Ultrasonic Reflection", *Experimental Mechanics, Proceedings of the 11th International Conference on Experimental Mechanics*, Balkema, Rotterdam, pp747-754.

Fernlund, I., 1970, "Druckverteilung zwischen Dichtflächen an verscrabten Flanschen", *Konstuktion*, Vol. 22, No. 6, pp218-224.

Fischer, G., Grubisic, V., Widmayer, H., 1988, "Fatigue Tests on Wheelsets under Simulated Service Strength Spectra", *Proceedings of the 9th International Wheelset Congress*, Montreal.

Hodgson, K., 2002. *The Use of Ultrasound to Investigate Engineering Contacts*, Phd Thesis, University of Sheffield.

Ito, Y., Toyoda, J.M. Nagata, S., 1977, "Interface Pressure Distribution in a Bolt-Flange Assembly", ASME Paper No. 77-WA/DE-11.

Johnson, K.L., 1985, *Contact Mechanics*, Cambridge University Press.

Kendall, K. and Tabor, D., 1971, An Ultrasonic Study of the Area of Contact between Stationary and Sliding Surfaces", *Proceedings of the Royal Society, Series A*, Vol. 323, pp321-340.

Lewis, R., Marshall, M.B., Dwyer-Joyce, R.S., 2002, Ultrasonic Characterisation of an Interference Fit, *Proceedings of the 29th Leeds-Lyon Symposium*, In Press.

Little, R.E., 1967, "Bolted Joints: How Much Give?", *Machine Design*, November 9th.

Mitsunaga, K., 1965, "The Pressure Distributions Between Bolted Plates (on the Stiffness Factors)", Transactions of the JSME, Vol. 31, No. 231, pp1750-1757.

Osgood C.C., 1979, "Saving Weight on Bolted Joints", *Machine Design*, October 25th.

Tattersall, A.G., 1973, "The Ultrasonic Pulse-Echo Technique as Applied to Adhesion Testing", *J. Phys. D: Appl. Phys*, Vol. 6, pp819-832.

Thomas, T.R. Sayles, R.S., 1977, "Stiffness of Machine Tool Joints: A Random-Process Approach", *Trans. ASME, J. Eng. Ind.*, Paper No. 76-WA/Prod-23.

Shibahara, M., Oda, J., 1969, "On Clamping Stiffness of Abutments in Bolted Joints", *Transactions of the JSME*, Vol. 72, No. 611, pp1611-1619.

Shigley, J.E., Mischke, C.R., 2001, *Mechanical Engineering Design*, Sixth Edition McGraw-Hill, Singapore.

Ziada, H.H., Abd El Latyif, A.K., 1980, "Loads, Pressure Distribution and Contact Area in Bolted Joints"